

# Low-Threshold Pump Power and High Integration in $\text{Al}_2\text{O}_3 : \text{Er}^{3+}$ Slot Waveguide Lasers on SOI

P. Pintus, *Student Member, IEEE*, S. Faralli, and F. Di Pasquale, *Member, IEEE*

**Abstract**—We numerically investigate the potential of  $\text{Al}_2\text{O}_3 : \text{Er}^{3+}$  active slot waveguides for realizing small-form factor lasers on silicon-on-insulator. Based on recent technological improvements in the reliable and low-cost fabrication of alumina doped with high  $\text{Er}^{3+}$  concentration, we point out the possibility of realizing silicon compatible emitters at  $1.55 \mu\text{m}$ , optically pumped at  $1480 \text{ nm}$  with a few milliwatts threshold pump power.

**Index Terms**—Slot waveguide, integrated optics, erbium, aluminum oxide.

## I. INTRODUCTION

SILICON is the dominating material for the electronics industry due to its good electrical properties and available mature and low-cost Si very large scale integration (VLSI) and complementary metal–oxide–semiconductor (CMOS) technology. Although it is a good material for passive optical waveguides at around  $1550 \text{ nm}$ , its indirect band-gap makes its use very challenging for achieving optical gain. In order to overcome this issue, several approaches have been investigated, like the use of silicon nano-clusters [1], [2]. However, only two solutions seem to be effective for realizing CMOS compatible lasers and optical amplifiers: hybrid integration of III–V semiconductors and silicon, and rare-earth-doped dielectric waveguides.

Although hybrid integration, in which electrically pumped AlGaInAs quantum-well materials are bonded on silicon waveguide structures [3], is attractive in terms of compactness, this approach is still very expensive and, in addition, III–V semiconductor-based amplifiers would likely suffer from cross-gain modulation effects [4] due to the short carrier lifetime of the active material. On the other hand, the relative low gain coefficient achievable in  $\text{Er}^{3+}$ -doped silica (lower than  $1 \text{ dB/cm}$  [5]) makes laser and amplifier integration difficult when using low index contrast silica-based waveguides.

In this letter, we propose the use of  $\text{Al}_2\text{O}_3 : \text{Er}^{3+}$  active slot waveguides for realizing small-form factor lasers on silicon-on-insulator (SOI); the high index contrast and superior gain (up to  $2 \text{ dB/cm}$  [6]) achievable in such a waveguide ensure strong field confinement and a small form factor [7], [8]. Our finite-element method (FEM)-based simulations use realistic parameters of the active material, which can be fabricated by low-cost cosputtering of  $\text{Al}_2\text{O}_3 : \text{Er}^{3+}$  [9], and they clearly point out the potential integration of CMOS compatible lasers, characterized by a few milliwatts (mW) threshold pump power at  $1480 \text{ nm}$ .

Manuscript received March 11, 2010; revised May 21, 2010; accepted June 12, 2010. Date of publication June 28, 2010; date of current version September 06, 2010.

The authors are with Scuola Superiore Sant'Anna, 56124, Pisa, Italy (e-mail: p.pintus@sssup.it; s.faralli@sssup.it; and f.dipasquale@sssup.it).

Color versions of one or more of the figures in this letter are available online at <http://ieeexplore.ieee.org>.

Digital Object Identifier 10.1109/LPT.2010.2054072

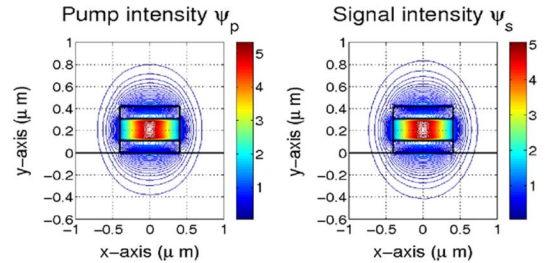


Fig. 1. Normalized power intensity profiles at pump wavelength ( $1480 \text{ nm}$ ) and signal wavelength ( $1534 \text{ nm}$ );  $\psi_p$  and  $\psi_s$  are in  $\mu\text{m}^{-2}$ .

Pumping at  $1480 \text{ nm}$  avoids the excess  $980\text{-nm}$  pump absorption due to the silicon layers forming the slot waveguide, but also leads to a significant influence of excited state absorption (ESA) on the laser output power.

## II. THEORETICAL MODEL

Considering the recent development of a new fabrication method for low-cost cosputtering deposition of  $\text{Al}_2\text{O}_3 : \text{Er}^{3+}$  [9], we have designed a slot waveguide laser based on this material. Two high refractive index silicon regions ( $n = 3.48$ ) clamp a thin highly erbium-doped alumina layer ( $n = 1.65$ ). The full structure is buried in a silica coating ( $n = 1.46$ ).

The electromagnetic analysis of our structure is based on a full vectorial FEM [10]. Numerical modes computation has been performed for the slot waveguide under investigation, which is schematically shown in Fig. 1; the same figure also reports the normalized intensity profiles at the pump and laser wavelengths,  $\psi_p$  and  $\psi_s$ , computed on the transversal waveguide cross-section.

The propagation equations, describing the longitudinal power evolution of the  $1480\text{-nm}$  pump, of the spectrally resolved amplified spontaneous emission (ASE) and lasing light at  $1534 \text{ nm}$ , are coupled with the steady-state population rate equations. Numerical solution is performed using the Runge–Kutta method. The power propagation equations for pump  $P_p$  are

$$\frac{dP_p}{dz} = P_p(z) \int_A [\sigma_{21}^p n_2 - \sigma_{12}^p n_1 - \sigma_{24}^p n_2] \cdot \psi_p dA - l_p P_p(z) \quad (1)$$

while the power propagation equations for copropagating and counterpropagating ASE lights ( $P_{\text{ASE}}^+$  and  $P_{\text{ASE}}^-$ ) are

$$\begin{aligned} \frac{dP_{\text{ASE}}^\pm}{dz} = & \pm P_{\text{ASE}}^\pm(z) \int_A [\sigma_{21}^s n_2 - \sigma_{12}^s n_1 - \sigma_{24}^s n_2] \cdot \psi_s dA \\ & \pm h\nu_s \Delta v \int_A \sigma_{21}^s n_2 \psi_s dA \mp l_s P_{\text{ASE}}^\pm(z). \end{aligned} \quad (2)$$

In (1) and (2),  $A$  is the transverse area of the active region (the lower refractive index region of the slot waveguide);  $\sigma_{12}^s$ ,  $\sigma_{21}^s$  are the spectral absorption and emission cross-sections within

the Er gain bandwidth;  $\sigma_{12}^p, \sigma_{21}^p$  are the absorption and emission cross-sections at the pump wavelength,  $l_p = l_s$  describe the background losses at both pump and ASE wavelengths. The equivalent input noise bandwidth  $\Delta\nu$  is assumed to be 0.1 nm, of the same order of the Bragg grating mirror reflectivity used at the laser cavity output. The model also includes ESA coefficients  $\sigma_{24}^p, \sigma_{24}^s$  from the Er<sup>3+</sup> meta-stable level  ${}^4I_{13/2}$  to the level  ${}^4I_{9/2}$ . Er<sup>3+</sup> ions in alumina matrix have been modeled considering a four-level steady-state rate equations system

$$\frac{\partial n_1}{\partial t} = -(W_{12} + R_{12})n_1 + \left( \frac{1}{\tau_2} + n_2 C_{UP} + W_{21} + R_{21} \right) n_2 \quad (3)$$

$$\frac{\partial n_2}{\partial t} = - \left( \frac{1}{\tau_2} + 2n_2 C_{UP} + W_{21} + R_{21} + W_{24} + R_{24} \right) n_2 + (W_{12} + R_{12})n_1 + \frac{n_3}{\tau_3} \quad (4)$$

$$\frac{\partial n_3}{\partial t} = -\frac{n_3}{\tau_3} + \frac{n_4}{\tau_4} \quad (5)$$

$$N_{Er} = n_1 + n_2 + n_3 + n_4 \quad (6)$$

where  $n_1, n_2, n_3,$  and  $n_4$  represent, respectively, the Er<sup>3+</sup> populations in the energy levels  ${}^4I_{15/2}, {}^4I_{13/2}, {}^4I_{11/2},$  and  ${}^4I_{9/2}$ ;  $N_{Er}$  is the total Er<sup>3+</sup> ions concentrations and  $\tau_i$  ( $i = 2, 3, 4$ ) are the state life times of the  ${}^4I_{13/2}, {}^4I_{11/2},$  and  ${}^4I_{9/2}$  levels ( $\tau_1: {}^4I_{13/2} \rightarrow {}^4I_{15/2}, \tau_2: {}^4I_{11/2} \rightarrow {}^4I_{13/2},$  and  $\tau_4: {}^4I_{9/2} \rightarrow {}^4I_{11/2}$ ). All rate equation parameters of Er<sup>3+</sup>-doped Al<sub>2</sub>O<sub>3</sub> are realistic values taken from the literature and reported in Table I. Equations (1), (2), and (3)–(6) are coupled through the induced transition rates  $R_{ij}$  and  $W_{ij}$

$$R_{ij} = \frac{\sigma_{ij}^p(\nu_p) I_p}{h\nu_p} \quad (7)$$

$$W_{ij} = \sum_{k=1}^m \frac{\sigma_{ij}^s(\nu_k)}{h\nu_k} [I_{ASE+} + I_{ASE-}] \quad (8)$$

where  $m$  is the number of slots used to discretize the gain bandwidth. The cavity is considered nonresonant at the pump wavelength and mono-modal at the lasing wavelength (we assumed an input dielectric mirror and an output Bragg reflector). Hence, the laser radiation boundary conditions are  $P_{ASE}^-(L, \nu_s) = R_2 P_{ASE}^+(L, \nu_s)$  and  $P_{ASE}^+(0, \nu_s) = R_1 P_{ASE}^-(0, \nu_s)$ , where  $R_1$  and  $R_2$  are the input and output mirror reflectivities,  $\nu_s$  is the laser frequency, and  $L$  is the cavity length. Due to a very short cavity, we can realistically assume a single longitudinal mode within the narrow Bragg reflector bandwidth, also expecting a narrow laser linewidth [11].

### III. NUMERICAL RESULTS

The slot waveguide has been carefully designed to be single mode at both pump and signal wavelengths and to maximize the field confinement on the active region (see Table II). The computed normalized intensity profiles are shown in Fig. 1.

Because of the high absorption coefficient in silicon at 980 nm [12], we have decided to pump the active material at 1480-nm wavelength. Pump light can be coupled into the active slot waveguide by means of integrated tapers or Bragg grating couplers

TABLE I  
PARAMETERS OF Er-DOPED Al<sub>2</sub>O<sub>3</sub>

Parameter	Value	Reference
$\sigma_{12}^p(1480nm)$	$3.27 \times 10^{-25} m^2$	Bradley et al. 09 [6]
$\sigma_{21}^p(1480nm)$	$1.10 \times 10^{-25} m^2$	Bradley et al. 09 [6]
$\sigma_{12}^s(1534nm)$	$5.73 \times 10^{-25} m^2$	Bradley et al. 09 [6]
$\sigma_{21}^s(1534nm)$	$5.74 \times 10^{-25} m^2$	Bradley et al. 09 [6]
$\sigma_{24}^p = \sigma_{24}^s$	$0.25 \times 10^{-25} m^2$	Kik et al. 03 [16]
$\sigma_{24}^p = \sigma_{24}^s$	$0.85 \times 10^{-25} m^2$	Hoven et al. 96 [17]
${}^4I_{13/2}$ life time $\tau_2$	8.6 ms	Bradley et al. 09 [6]
${}^4I_{11/2}$ life time $\tau_3$	30 $\mu s$	Hoven et al. 96 [18]
${}^4I_{9/2}$ life time $\tau_4$	1 ns	Chryssou et al. 01 [19]
$C_{up}(N_{Er}=4.22 \times 10^{26} ions/m^3)$	$1.0 \times 10^{-23} m^3/s$	Bradley et al. 09 [6]

\*We have used the lowest and more recent value for ESA coefficients.

TABLE II  
SLOT GEOMETRICAL PARAMETERS

Parameter	Width	Thickness	Material	Refractive Index
Slot	800 nm	200 nm	Al <sub>2</sub> O <sub>3</sub> :Er <sup>3+</sup>	1.65
High Refractive Index Layers	800 nm	110 nm	Si	3.48

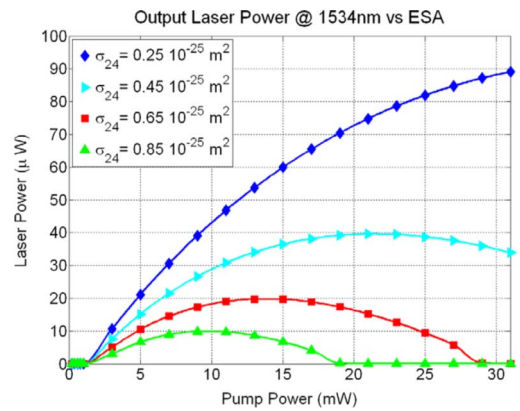


Fig. 2. Laser output power versus pump power. ESA seriously affects output laser power. The cavity is 7 mm long,  $R_2 = 0.97$  and  $N_{Er} = 4.22 \times 10^{26}$  ions/m<sup>3</sup>.

[13]. We assumed a background loss of 1 dB/cm; although this value is rather low for slot waveguides, it is a realistic value due to recent technological improvements [14], [15] and low material loss [9]. Considering an Er<sup>3+</sup> concentration of  $4.22 \times 10^{26}$  ions/m<sup>3</sup> [6],  $R_1 = 0.999$ ,  $R_2 = 0.97$  and a 7-mm cavity, we have investigated how ESA affects the lasing output power, which is computed as  $P_{out}(\nu_s) = (1 - R_2) \cdot P_{ASE}^+(L, \nu_s)$ .

Fig. 2 reports the laser output power versus input pump power for different ESA cross-section values; by increasing the ESA cross-sections  $\sigma_{24}^p$  and  $\sigma_{24}^s$  from  $0.25 \times 10^{-25} m^2$  [16] to  $0.85 \times 10^{-25} m^2$  [17], we can clearly see that the laser output power is seriously reduced. Note that the impact of ESA, which is negligible in standard erbium-doped fiber amplifiers (EDFAs) and erbium-doped waveguide amplifiers (EDWAs), becomes important in Er<sup>3+</sup>-doped slot waveguides due to the extremely high power confinement achievable in such structures. We can also clearly see an optimum input pump power above which the output lasing light starts to decrease due to a strong ESA-induced population of the  ${}^4I_{11/2}$  Er<sup>3+</sup> level. Considering the most recently measured and more optimistic values for  $\sigma_{24}^p$  and  $\sigma_{24}^s$  [16], we have then optimized the laser cavity length in order to

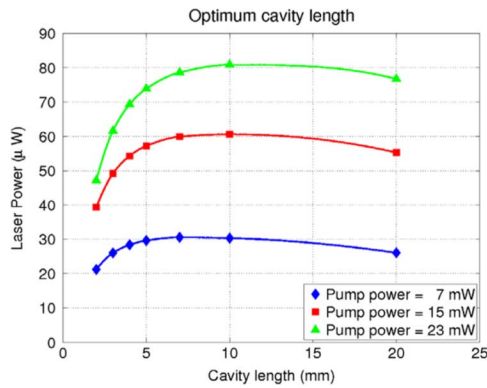


Fig. 3. Laser output power versus the waveguide length, for different pump powers: 7, 15, and 23 mW,  $R_2 = 0.97$  and  $N_{Er} = 4.22 \times 10^{26}$  ions/m<sup>3</sup>.

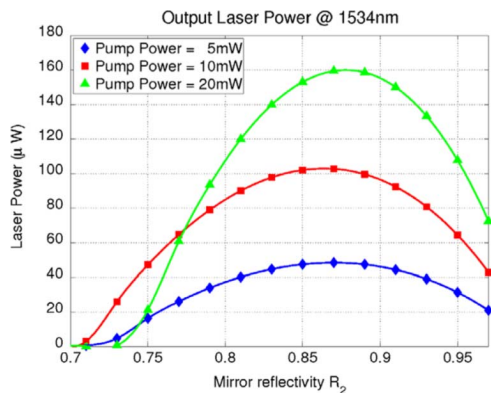


Fig. 4. Laser output power versus output mirror reflectivity  $R_2$ , for different pump powers: 5, 10, and 20 mW.

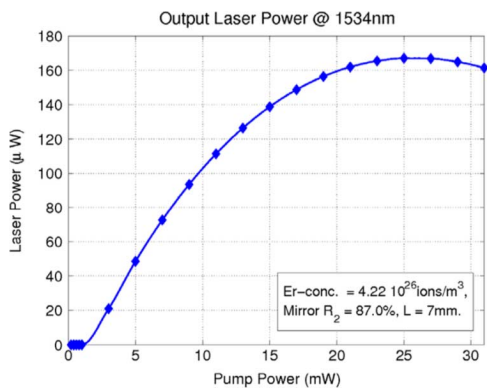


Fig. 5. Laser output power versus pump power. The cavity is 7 mm long,  $R_2 = 0.87$ , and  $N_{Er} = 4.22 \times 10^{26}$  ions/m<sup>3</sup>.

maximize the laser output power at 1534 nm. Fig. 3 shows that a 7-mm-long cavity allows us to realize an effective device integration with significant and optimized output power. Finally, we have varied the output mirror reflectivity for maximizing the output laser power; this analysis is shown in Fig. 4, where we can clearly note an optimum value of approximately 0.87. With such optimized output mirror reflectivity ( $R_2 = 0.87$ ) and waveguide length (7 mm), we have finally investigated the lasing output power versus input pump power; the results reported in Fig. 5 clearly show that more than 100- $\mu$ W output lasing power can be realistically achieved with less than 10-mW pump power. We can also note a few mW laser pump threshold and limited output laser degradation due to ESA effect.

## IV. CONCLUSION

We have numerically demonstrated the potential of an active slot waveguide in  $\text{Al}_2\text{O}_3:\text{Er}^{3+}$  for CMOS compatible small-form factor integrated laser with a few mW threshold pump power at 1480 nm. Even if ESA may affect the laser output power, we believe that the low-cost fabrication technique [9], combined with possible use of broad-area lasers to simultaneously pump active slot waveguide arrays, can lead to attractive components and significantly reduce the cost of integration.

## REFERENCES

- [1] G. T. Reed, *Silicon Photonics, the State of the Art*. Hoboken, NJ: Wiley, 2008.
- [2] M. Cazzanelli, D. Navarro-Urriós, F. Riboli, N. Daldosso, and L. Pavesi, "Optical gain in monodispersed silicon nanocrystals," *J. Appl. Phys.*, vol. 96, no. 6, pp. 3164–3171, Sep. 15, 2004.
- [3] A. W. Fang, H. Park, O. Cohen, R. Jones, M. J. Paniccia, and J. E. Bowers, "Electrically pumped hybrid AlGaInAs-silicon evanescent laser," *Opt. Express*, vol. 14, no. 20, pp. 9203–9210, 2006.
- [4] P. S. Cho and J. B. Khurgin, "Suppression of cross-gain modulation in SOA using RZ-DPSK modulation format," *IEEE Photon. Technol. Lett.*, vol. 15, no. 1, pp. 162–164, Jan. 2003.
- [5] K. Hattori, T. Kitagawa, M. Ogum, Y. Ohmori, and M. Horiguchi, "Erbium-doped silica-based waveguide amplifier integrated with 980/1530 nm WDM coupler," *Electron. Lett.*, vol. 30, no. 11, pp. 856–857, 1994.
- [6] J. Bradley, L. Agazzi, D. Geskus, F. Ay, K. Wörhoff, and M. Pollnau, "Gain bandwidth of 80 nm and 2 dB/cm peak gain in  $\text{Al}_2\text{O}_3:\text{Er}^{3+}$  optical amplifiers on silicon," *J. Opt. Soc. Amer. B*, vol. 27, no. 2, pp. 187–196, 2010.
- [7] V. R. Almeida, Q. Xu, C. A. Barrios, and M. Lipson, "Guiding and confining light in void nanostructure," *Opt. Lett.*, vol. 29, no. 11, pp. 1209–1211, 2004.
- [8] R. Sun, P. Dong, N. Feng, C. Hong, J. Michel, M. Lipson, and L. Kimerling, "Horizontal single and multiple slot waveguides: Optical transmission at  $\lambda = 1550$  nm," *Opt. Express*, vol. 15, no. 26, pp. 17967–17972, 2007.
- [9] K. Wörhoff, J. D. B. Bradley, F. Ay, D. Geskus, T. P. Blauwendraat, and M. Pollnau, "Reliable low-cost fabrication of low-loss  $\text{Al}_2\text{O}_3:\text{Er}^{3+}$  waveguides with 5.4-dB optical gain," *IEEE J. Quantum Electron.*, vol. 45, no. 5, pp. 454–461, May 2009.
- [10] J. Jin, *The Finite Element Method in Electro-Magnetics*. Hoboken, NJ: Wiley, 2002.
- [11] W. H. Loh, B. N. Samson, L. Dong, G. J. Cowle, and K. Hsu, "High performance single frequency fiber grating-based erbium/ytterbium-codoped fiber lasers," *J. Lightw. Technol.*, vol. 16, no. 1, pp. 114–118, Jan. 1998.
- [12] M. A. Green and M. Keevers, "Optical properties of intrinsic silicon at 300 K," *Progress in Photovoltaics*, vol. 3, no. 3, pp. 189–192, 1995.
- [13] J. V. Galan, P. Sanchis, J. Blasco, and J. Marti, "Horizontal slot waveguide based efficient fiber couplers for silicon photonics," in *Proc. Eur. Conf. Integrated Optics (ECIO'08)*, Eindhoven, The Netherlands, Jun. 11–13, 2008, Paper ThP16.
- [14] K. Preston and M. Lipson, "Slot waveguides with polycrystalline silicon for electrical injection," *Opt. Express*, vol. 17, no. 3, pp. 1527–1534, 2009.
- [15] R. M. Pafchek, J. Li, R. S. Tummid, and T. L. Koch, "Low loss Si-SiO<sub>2</sub>-Si 8-nm slot waveguides," *IEEE Photon. Technol. Lett.*, vol. 21, no. 6, pp. 353–355, Mar. 15, 2009.
- [16] P. G. Kik and A. Polman, "Cooperative upconversion as the gain-limiting factor in Er doped miniature  $\text{Al}_2\text{O}_3$  optical waveguide amplifiers," *J. Appl. Phys.*, vol. 93, no. 9, pp. 5008–5012, May 1, 2003.
- [17] G. N. van den Hoven, R. J. I. M. Koper, A. Polman, C. van Dam, J. W. M. van Uffelen, and M. K. Smit, "Net optical gain at 1.53  $\mu\text{m}$  in Er-doped  $\text{Al}_2\text{O}_3$  waveguides on silicon," *Appl. Phys. Lett.*, vol. 68, no. 14, pp. 1886–1888, 1996.
- [18] G. N. van den Hoven, E. Snoeks, A. Polman, C. van Dam, J. W. M. van Uffelen, and M. K. Smit, "Upconversion in Er-implanted  $\text{Al}_2\text{O}_3$  waveguides," *J. Appl. Phys.*, vol. 79, no. 3, pp. 1258–1266, 1996.
- [19] C. E. Chrystou, F. Di Pasquale, and C. W. Pitt, "Improved gain performance in Yb<sup>3+</sup>-sensitized Er<sup>3+</sup>-doped alumina ( $\text{Al}_2\text{O}_3$ ) channel optical waveguide amplifiers," *J. Lightw. Technol.*, vol. 19, no. 3, pp. 345–349, Mar. 2001.